Polymer Chemistry

PAPER

View Article Online
View Journal

Cite this: DOI: 10.1039/c5py01852h

Stimuli-responsive supramolecular materials: photo-tunable properties and molecular recognition behavior†

Cheng-Wei Huang,[a] Pei-Wei Wu,[b] Wei-Hung Su,[b] Chao-Yuan Zhu*[a] and Shiao-Wei Kuo*[b]

Received 19th November 2015,
Accepted 30th November 2015

DOI: 10.1039/c5py01852h

www.rsc.org/polymers

A new homopolymer of polystyrene (PS) presenting pendant diaminopyridine (DAP) moieties has been prepared using controlled free radical polymerization and a CuAAC "click" reaction. Through directional complementary multiple hydrogen bonding, this PVB-DAP polymer underwent complexation with a thymine-functionalized azobenzene (Azo-T). The resulting supramolecular complex exhibited amorphous and chromophoric behavior without microphase separation. This strategy allowed the fabrication of homogeneous stimuli-responsive thin films with photocontrollable behavior through photoinduced *trans–cis* isomerization. The PVB-DAP/Azo-T supramolecular complex facilitated the dispersion of an azo-dye through noncovalent interactions; the resulting complex was used to fabricate a surface relief grating displaying an interference pattern. The "recordability" and "rewritability" of these supramolecular complexes suggest that they are promising materials for optical applications and therefore advance the pathway for supramolecular development.

Introduction

Stimuli-responsive materials have attracted much attention for their potential applications in biomedical science,[1] for switchable adhesion,[2] and for micro- and nanoactuation.[3] A recent surge in interest in these "smart materials" has been focused on their unique ability to modulate the surface properties and self-assembly phenomena.[4] Polymers, lipids, and other macromolecules are often used in fundamental and applied chemical explorations of smart materials;[5] in particular, polymers are most commonly examined because of their flexibility in terms of material design. The availability of many polymerization strategies [*e.g.*, atom transfer radical polymerization (ATRP), nitroxide mediated radical polymerization (NMP), reversible addition–fragmentation chain transfer polymerization (RAFT), and ring-opening polymerization (ROP)] makes polymeric materials easy to synthesize and possible to form as special types of block copolymers.[6] Graft copolymers have a promising future because of the possibility of post-functionalizing them after polymerization. Since the concept of click chemistry was first demonstrated by Sharpless *et al.*,[7] several click reactions, including copper(I)-catalyzed alkyne–azide cycloaddition (CuAAC), Diels–Alder reactions, and thiol–ene reactions, have been developed for use in polymer synthesis. Many efforts have been made to design responsive polymeric materials that are easy to synthesize and display good processability.

Supramolecular chemistry, a concept inspired by Nature, is a useful protocol for molecular design. Highly ordered self-assembled structures can be obtained that are stabilized through noncovalent interactions, commonly hydrogen bonding, coordination, ionic, and π–π interactions.[8] Hydrogen-bonded supramolecular materials have been the most widely examined as a result of the selectivity and directionality of hydrogen bonds.[9] The stability of a hydrogen-bonded complex can be tuned by altering the molecular recognition behavior of complementary base pairs. A typical example is the self-assembly of the DNA duplex, a unique structure formed with the assistance of adenine (A), thymine (T), cytosine (C), and guanine (G) bases. More interestingly, chemists have used such interactions to prepare series of organic molecules as biomimetic structures that extend the applicability of traditional polymers.[10] Post-functionalized hydrogen-bonded donor/acceptor motifs can effectively connect two immiscible organic/inorganic compounds into a miscible complex and, thereby, modulate the individual thermal and photoelectric properties.[11]

[a]*Institute of Applied Chemistry, National Chiao Tung University, HsinChu, 300, Taiwan. E-mail: cyzhu@mail.nctu.edu.tw*
[b]*Department of Materials and Optoelectronic Science, Center for Nanoscience and Nanotechnology, National Sun Yat-Sen University, Kaohsiung, 804, Taiwan. E-mail: kuosw@faculty.nsysu.edu.tw*

†Electronic supplementary information (ESI) available. See DOI: 10.1039/c5py01852h

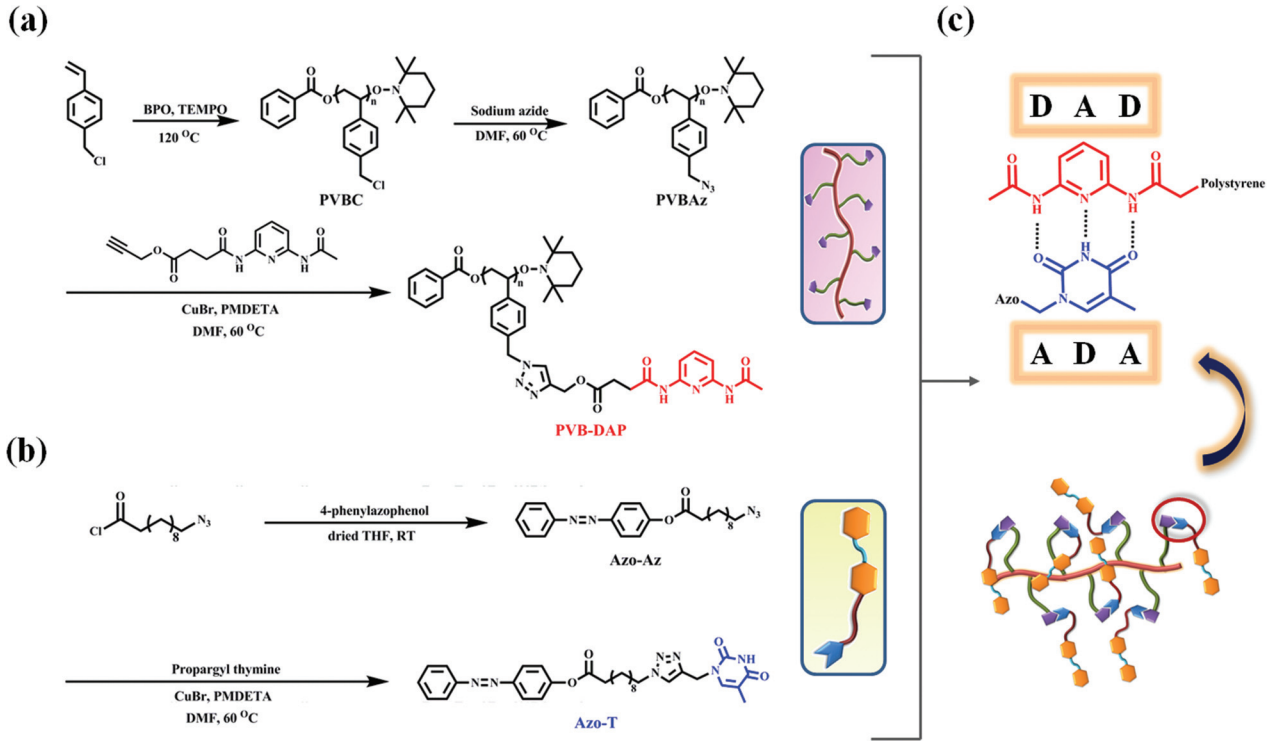

Scheme 1 Synthesis of (a) PVB-DAP and (b) Azo-T and (c) an illustration of a hydrogen-bonded base pair.

The photochemistry of azobenzene is a fascinating process for the applications of many supramolecular complexes. Azo-chromophores are versatile molecules that are relatively robust and chemically stable. Their most intriguing phenomenon is *trans–cis* isomerization under ultraviolet (UV) or visible light. The photoresponsive nature of azobenzenes can result in remarkable variations in the molecular orientation, dipole moments, and visual color.[12] These geometric changes allow the materials incorporating azo molecules to be used in, for example, host/guest applications,[13] as light-triggered nano-carriers,[14] in micropatterning,[15] and as optical storage media.[16] Photo-addressable azo-functionalized polymers have been developed for data storage and polarization holography. Another promising application is microscopic mass transport, induced under illumination with linearly polarized light and erased under irradiation with circularly or non-polarized light.[17] Accordingly, azo-containing polymers are good candidates for use in holographic storage. Unfortunately, some azo-polymers display poor stability, as a result of rather low glass transition temperatures (T_g), in the form of amorphous copolymers.[17,18] Thus, the thermal properties of responsive materials should be considered during material design. Moreover, another criterion for photoinduced mass migration is sufficiently strong interactions between the polymer backbone and the chromophores. Therefore, covalent and noncovalent (*e.g.*, ionic or hydrogen bonding interactions) functionalization should be considered during molecular design.[19,20]

In this study, we developed a new supramolecular system taking the advantage of complementary multiple hydrogen bonding between T and diaminopyridine (DAP) base pairs (Scheme 1). Controlled free radical polymerization allowed the simple and efficient preparation of a polymer matrix presenting modifiable functionalities on its side chains. A subsequent copper-catalyzed click reaction provided a graft polymer incorporating strongly hydrogen bonding moieties capable of forming supramolecular architectures. The combination of a noncovalent network and stimuli-responsive azo molecules provided new derivatives possessing good miscibility and tunable thermal and photophysical properties. Indeed, we used this approach to form materials with unique surface structures. To the best of our knowledge, this paper reports the first micro-patterned structure constructed from a photochemically/thermally responsive multiple-hydrogen-bonded supramolecular complex. We have examined the water contact angles (WCAs) of these surfaces and their use in the generation of surface relief gratings (SRGs).

Experimental section

Materials

4-Vinylbenzyl chloride (VBC; Aldrich) was distilled from CaH_2 under reduced pressure. Propargyl bromide (80% in toluene, stabilized with MgO) was obtained from Alfa. All solvents were purchased from TEDIA (USA) and distilled over CaH_2 prior to use. Commercially available reagents were obtained from Sigma-Aldrich or Showa and used as received.

Characterization

Fourier transform infrared (FTIR) spectra were recorded using a Bruker Tensor 27 FTIR spectrometer; 32 scans were collected at room temperature at a resolution of 1 cm^{-1}; the regular KBr disk method was employed for sample preparation. ^{1}H and ^{13}C nuclear magnetic resonance (NMR) spectra of samples in $CDCl_3$, 1,1,2,2-tetrachloroethane-d_2, or DMSO-d_6 were recorded using a Varian UNITY INOVA 500 MHz spectrometer (equipped with a 11.75-T Bruker magnet) at 500 and 125 MHz, respectively. The association constant of the supramolecular complex was measured using NMR spectroscopy and solutions containing various ratios of SA-DAP and Azo-T. Variable-temperature NMR spectroscopy was conducted using a Varian VNMRS 600 MHz spectrometer (equipped with a 16.4-T Bruker magnet). Molecular weights and the polydispersity index (PDI) were measured using a Waters 510 gel permeation chromatography (GPC) system equipped with a refractive index detector and three Ultrastyragel columns (100, 500, and 1000 Å) connected in series. DMF was the eluent at a flow rate of 0.8 mL min^{-1} at 50 °C; the system was calibrated using polystyrene (PS) standards. Differential scanning calorimetry (DSC) was performed using a TA Instruments Q-20 apparatus under an atmosphere of dry N_2. The samples were weighed (3–5 mg) and sealed in an aluminum pan, and then scanned from −80 to +150 °C at a rate of 10 °C min^{-1}. Atomic force microscopy (AFM) was performed at 20 °C in air using a Dimension 3100 apparatus (Digital Instrument), operated in the tapping regime mode, equipped with silicon cantilever tips (PPP-NCH-50, 204–497 kHz, 10–130 N m^{-1}); the scan rate was 256 samples per line. UV-Vis spectra were recorded using an HP 8453 diode-array spectrophotometer. Sample irradiation was performed using a UVP CL-1000 UV cross-linker (UVP, Cambridge, UK) at 365 nm. Wide-angle X-ray scattering (WAXS) and small-angle X-ray scattering (SAXS) were performed using the BL17A1 wiggler beamline of the National Synchrotron Radiation Research Center (NSRRC), Taiwan. The samples were sealed between two Kapton windows (thickness: 12 μm) and measured at room temperature. An X-ray beam having a diameter of 0.5 mm and a wavelength of 1.1273 Å was used for the SAXS measurements (Q range: 0.015–0.3 A^{-1}). Optical microscopy (OM; Leica DM2500M) was used to observe the surface structure of the SRGs. The film thicknesses were measured using an N & K analyzer (n&k Analyzer 1280) with transparent glass substrates. The static WCAs were measured using a VCA Optima XE Dynamic Contact Angle Analyzer (AST Products, Billerica, MA) under ambient conditions; after the water drop had been deposited on the film surface, images were recorded immediately by a CCD camera; at least five measurements were averaged for each sample.

Complex preparation

Mixtures of PVB-DAP and Azo-T were prepared through solution-blending. A DMF solution containing 5 wt% of the polymer mixture was stirred for 24 h; the solvent was then evaporated slowly at room temperature. The resulting blend films were dried at 70 °C for another 24 h prior to measurement of their properties.

SRG fabrication

A dye-doped supramolecular thin film (500 nm) was prepared through a solution-blending method, as mentioned above. Polarized green light (532 nm) with an intensity of 20 mW cm^{-2} was prepared using a diode-pumped solid state (DPSS) laser. The laser light was collimated and passed through a polarized beam splitter. The incident angle of the reference beam was maintained at 3.5° in the air. A transverse electric (TE)-polarized He–Ne laser beam (632 nm) was chosen to probe the grating.

Results and discussion

Synthesis of DAP conjugated homopolymer

The functional polystyrene PVB-DAP capable of forming multiple hydrogen bonds was synthesized in three steps [Scheme 1(a)]. Nitroxide-mediated polymerization of VBC with TEMPO as the initiator resulted in the homopolymer PVBC, which was converted into the polyazide PVBAz through a reaction with sodium azide. The FTIR spectrum of PVBAz featured a new absorption peak at 2095 cm^{-1} (Fig. 1), characteristic of an organic azide. Fig. 2 presents the ^{1}H NMR spectra of PVBC and PVBAz. The broad signals at 7.2 and 6.8–6.2 ppm are related to the aromatic protons of the polystyrene structure. No obvious signals for a C=C double bond are evident in the spectrum of PVBC, indicating that its purity was high. The signal from PVBC at 4.5 ppm, representing its benzylic CH_2 groups, disappeared completely and a new signal appeared upfield (at 4.2 ppm) after incorporation of the N_3 groups. A click reaction then introduced the multiple-hydrogen-bonding functionality DAP. The NMR spectrum of the product,

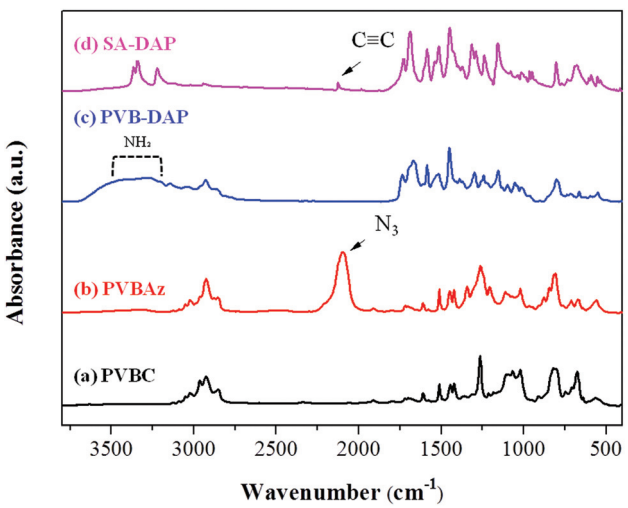

Fig. 1 FTIR spectra of (a) PVBC, (b) PVBAz, (c) PVB-DAP, and (d) SA-DAP.

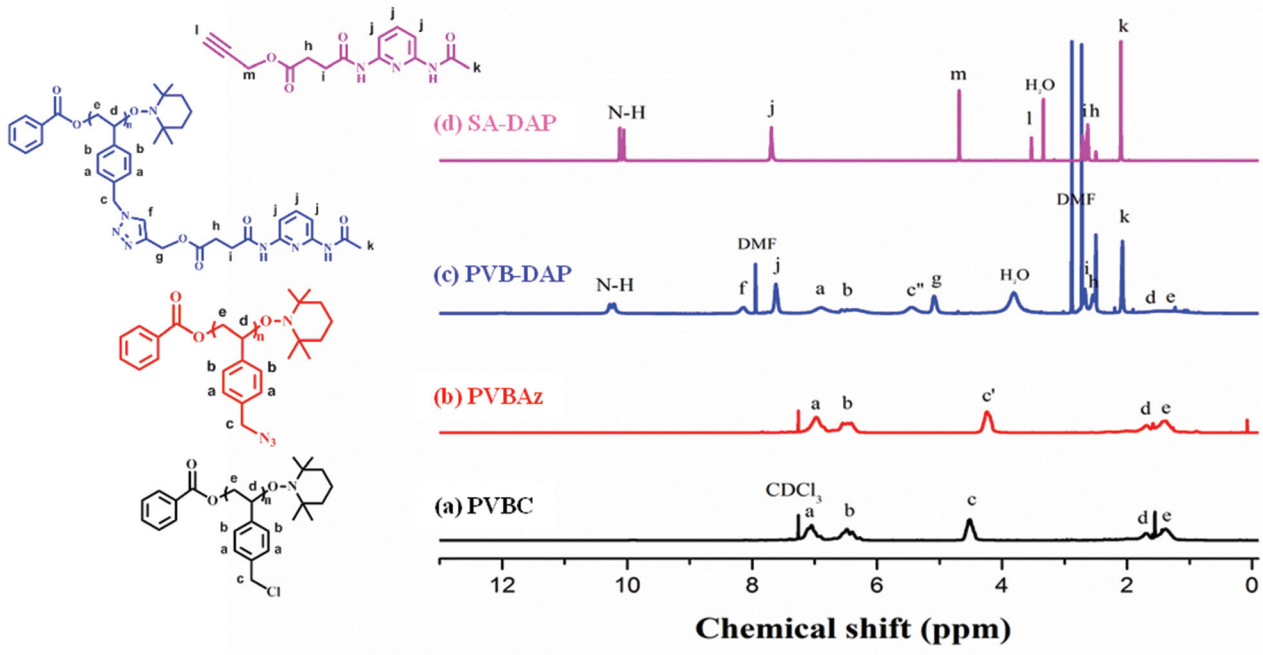

Fig. 2 ^{1}H NMR spectra of (a) PVBC and (b) PVBAz in $CDCl_3$ and of (c) PVB-DAP and (d) SA-DAP in DMSO-d_6.

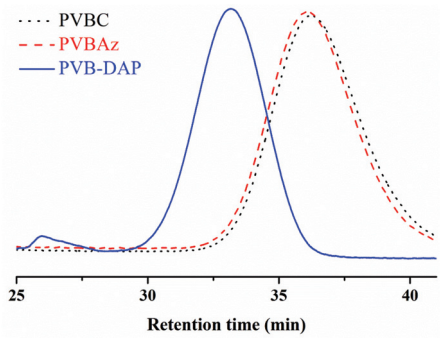

Fig. 3 GPC traces of PVBC, PVBAz, and PVB-DAP homopolymers.

Table 1 Characterization data for the homopolymers used in this study

Homopolymer	M_n [a]	M_w [b]	PDI [c]
PVBC	18 300	22 100	1.21
PVBAz	19 200	23 400	1.22
PVB-DAP	48 600	55 900	1.15

[a] Number-average molecular weight. [b] Weight-average molecular weight. [c] Polydispersity calculated from GPC traces.

PVB-DAP, featured two signals at 5.4 and 5.1 ppm representing the two types of CH_2 units neighboring the newly formed triazole rings. Similar phenomena were evident in the ^{13}C NMR spectra (Fig. S1†), with the signal of the benzylic CH_2 unit of PVBC shifting from 46.5 to 54.6 ppm after the formation of PVBAz, and then shifting to 57.7 ppm after the click reaction. During the click reaction, the signal at 2095 cm^{-1} for the azide decreased gradually and finally disappeared, consistent with PVB-DAP being formed. The combined FTIR and NMR spectral results confirmed that the Cu(I)-catalyzed click reaction was suitable for post-functionalization of this polystyrene derivative. We used GPC with DMF as the eluent to calculate the molecular weights of our homopolymers (Fig. 3, Table 1). Each one exhibited a narrow PDI (<1.22); therefore, in our subsequent experiments we could ignore the possibility of any interference from low-molecular-weight oligomers. The peak shape of the eluted PVBAz was similar to that of PVBC, with a slight shift toward a lower retention time (a higher molecular weight), consistent with their slightly different side chains. For PVB-DAP, however, we observed a dramatic change in the elution profile. After the side-chain click reaction with SA-DAP, the number-average molecular weight (M_n) increased from 19 200 to 48 600 Da. Furthermore, the GPC trace of PVB-DAP featured another small, broad peak at 25.5–28 min, possibly arising from aggregation through hydrogen bonding of the DAP units. These results are consistent with the synthesis of PVB-DAP, a polystyrene derivative containing 50% DAP units and capable of forming multiple hydrogen bonds with the complementary T units.

Synthesis of T-functionalized azobenzene

The T-functionalized azobenzene with a long alkyl spacer was readily synthesized in two steps [Scheme 1(b)]. 4-Phenylazophenol was first reacted with an aliphatic acid chloride to form 4-(phenyldiazenyl)phenyl-11-azidoundecanoate (Azo-Az),

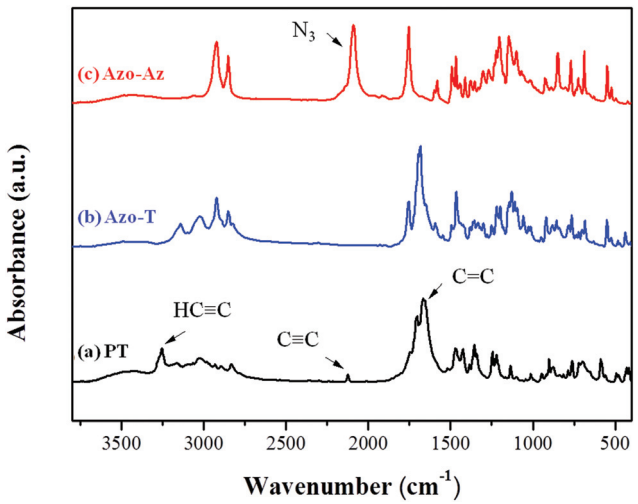

Fig. 4 FTIR spectra of (a) PT, (b) Azo-T, and (c) Azo-Az.

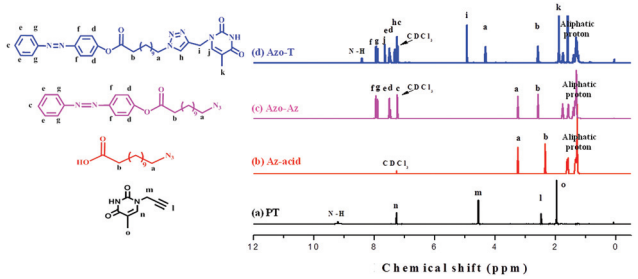

Fig. 5 ^{1}H NMR spectra of (a) PT, (b) Az-acid, (c) Azo-Az, and (d) Azo-T in $CDCl_3$.

which was then "clicked" with propargyl thymine to form Azo-T as a yellow powder in 90% yield. After the triazole ring formation with PT, the signal at 2090 cm^{-1} for the azide stretching in the FTIR spectrum of Azo-Az disappeared completely in the spectrum of Azo-T (Fig. 4). The CH_2 proton neighboring the C═O group shifted upfield from 2.34 to 2.58 ppm after acylation of the azophenol. In contrast, the signal of the CH_2 group neighboring the azide group remained unchanged after the reaction of the original aliphatic acid. After the click reaction, three characteristic signals of the triazole were present in the NMR spectrum (Fig. 5 and S2†): the two CH_2 groups beside the triazole unit provided signals at 4.93 ppm (singlet) and 4.31 ppm (triplet), respectively, while the signal of the proton on the triazole ring appeared at 7.3 ppm. The characteristic signal also appeared for the CON*H*CO and CC*H*$_3$ units of the T group at 8.41 and 1.89 ppm, respectively. Thus, the combined FTIR and NMR spectral data confirmed the successful functionalization of T.

Molecular recognition of PVB-DAP/Azo-T in the bulk state

Because of the specific hydrogen bonding between the DAP and T base pairs, the properties of their complexes can be controlled by varying their blending ratios.[21] We used FTIR spectroscopy to examine the interaction between the DAP and T functionalities. Fig. S3† reveals a signal for the T···T dimer of Azo-T at 3173 cm^{-1}.[22] The spectrum of PVB-DAP exhibited characteristic signals at 3407 cm^{-1} for free amide N–H stretching and 3269 and 3205 cm^{-1} for bound amide N–H stretching.[23] The presence of a signal for the free N–H units indicated that some of the DAP groups on the side chain of the polystyrene were not involved in hydrogen bonding interactions.[24] Upon increasing the content of Azo-T, the intensity of the signal at 3407 cm^{-1} decreased gradually upon the formation of DAP/T complexes. This finding suggests that the DAP···T interaction was stronger than the T···T and DAP···DAP interactions, as illustrated in Scheme 1(c). The signal for the T···T dimer interaction at 3173 cm^{-1} also decreased, due to the disruptive effects of the DAP units. Notably, the signal for the T···T dimer disappeared eventually, in contrast to its behavior reported previously,[25] indicating that the DAP···T interaction was sufficiently strong to break all of the T···T dimers and, thereby, form a highly assortative supramolecular complex.

In any blending system, the fractions of the components can control the thermal properties of the entire system.[26] To investigate the effects of different blending ratios, Fig. 6 presents DSC thermograms of our supramolecular complexes. PVB-DAP exhibited a clear glass transition at a value of T_g of 99.1 °C without any melting point, suggesting the amorphous nature of this polystyrene derivative. In contrast, Azo-T displayed a sharp melting point (T_m) of 175.3 °C, due to the strong crystallization ability of its azobenzene unit. Increasing the ratio of the complementary organic dye, Azo-T caused the value of T_g of the PVB-DAP/Azo-T complex to decrease gradually, implying the formation of a highly complementary supramolecular structure. The decrease in the value of T_g can be explained in terms of the plasticizing effect arising from the long alkyl spacer between the azobenzene and T moieties.[27] The supramolecular complex appeared strong molecular recognition behavior until the PVB-DAP/Azo-T ratio reached 1/1, the fraction at which the complex exhibited its lowest value of

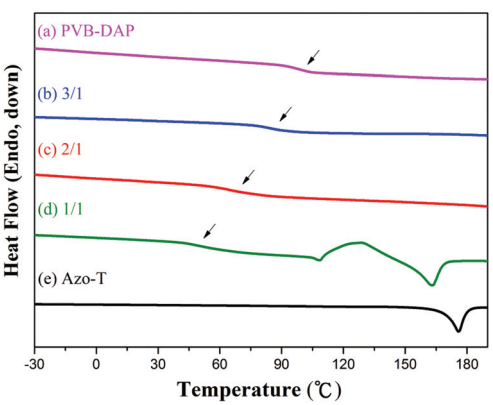

Fig. 6 DSC thermograms of (a) pure PVB-DAP; (b) 3/1, (c) 2/1, and (d) 1/1 PVB-DAP/Azo-T complexes; and (e) pure Azo-T.

T_g, indicating that strong noncovalent interactions existed between the DAP and T units; nevertheless, crystallization behavior was also apparent, with a signal appearing with a value of T_m of 163.1 °C. This result suggested that excess Azo-T was present in the complex, leading to the formation of a more regular crystalline phase.[28] In the DSC experiment we found that the ratios of 2/1 and 3/1 provided homogeneous supramolecular materials; therefore, we chose the materials formed at these ratios for subsequent experiments.

Binding affinity and thermal-responsiveness of the supramolecular complex

We expected interesting behavioral changes of our supramolecular complex as a result of its DAP···T interactions. To investigate the binding affinity of the units in the physical crosslinked structure, we performed a ^{1}H NMR spectroscopic titration experiment. We used the model compound SA-DAP, which has better solubility in chlorinated aprotic solvents, in the titration experiment as a proxy to monitor the interaction between PVB-DAP and Azo-T. In the NMR spectroscopic titration we systematically increased the SA-DAP concentration from 15 to 145 mM in 1,1,2,2-tetrachloroethane-d_2 and measured the spectra at 25 °C. Using this approach, we calculated the association constant (K_a) from the titration data (Fig. 7 and S4). One piece of evidence for heteromeric hydrogen bonding interaction was a shift in the position of the signal for the nucleobase imide unit.[29] The signals of the amido NH units also became broader relative to those of the original material, implying that a rapid exchange occurred between intermolecular association and dissociation on the measured time scale. The value of K_a for this supramolecular system was 31.5 M^{-1}, calculated using the Benesi–Hildebrand mathematical model.[29] The strong cooperative interaction through complementary hydrogen bonding led to a special morphological variability in solution and in the bulk state.

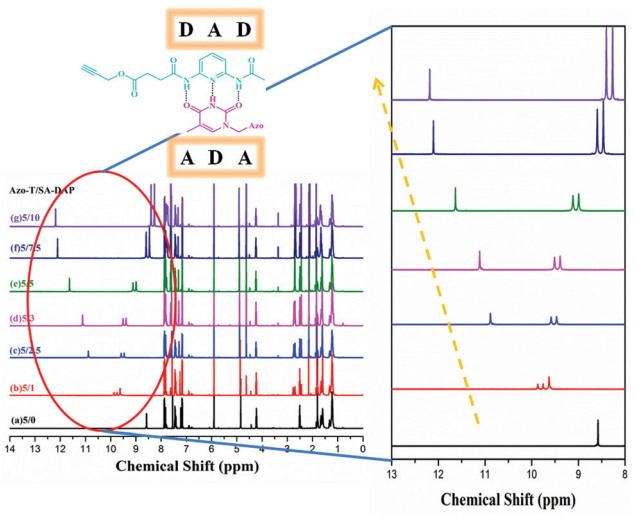

Fig. 7 ^{1}H NMR titration spectrum of the Azo-T/SA-DAP complex.

Indeed, the combination of two immiscible compounds formed a homogeneous state and retained the merits of both materials.

Hydrogen-bonded supramolecular complexes are attractive materials because their dynamic interactions and thermo-responsivity are unique properties not found in covalently bonded materials. Variable-temperature ^{1}H NMR spectroscopy is a useful technique for examining the stimuli-responsivity (*e.g.*, temperature-dependence) of hydrogen-bonded association/dissociation processes.[30] Fig. 8 displays the variation in the chemical shift of the NH unit of the DAP···T complex at a ratio of 5/7.5 in 10 wt% 1,1,2,2-tetrachloroethane-d_2 upon changing the temperature. The original peak was positioned at 12.11 ppm at 25 °C, suggesting a strongly complementary interaction. As the temperature increased, the signal of the NH unit shifted upfield, broadening gradually and reaching 10.18 ppm at 100 °C. This temperature-dependent behavior implies partial dissociation of the DAP···T base pairs.[29,31] The signal for the NH unit shifted back to its original position (12.11 ppm) after cooling the sample from 100 to 25 °C. This supramolecular complex exhibited thermo-responsivity and reversibility because of its stable DAP···T hydrogen bonds. Variable-temperature FTIR spectroscopy is another common method for monitoring the behavior of supramolecular complexes. In Fig. S5,† we assign the peaks centered at 3269 and 3205 cm^{-1} to the bound NH units in the complex. Upon increasing the temperature from 25 to 160 °C, the signals at 3269 and 3205 cm^{-1} shifted to slightly higher wavenumbers and broadened. In addition, a signal for free amide NH units appeared near 3400 cm^{-1}; its intensity increased upon increasing the temperature, indicative of thermal dissociation of the DAP···T base pairs.[32] The spectrum returned to its original state after cooling from 160 to 25 °C. The phenomena of thermoresponsivity and reversibility, endowed by strong noncovalent supramolecular interactions, are consistent with those observed in the variable-temperature ^{1}H NMR spectra.

Photoresponsivity of azobenzene-contained supramolecular complex

Azobenzene is well known for its stimuli-responsive behavior. To investigate the photoresponsivity of our PVB-DAP/Azo-T supramolecular complex, we measured its UV-Vis spectrum before and after UV irradiation at 365 nm and recorded the results until the photostationary state had been reached. Fig. 9(a) reveals that the intensity of the absorbance near 327 nm (π–π*) decreased while those of the bands at 263 and 435 nm (n–π*) increased gradually. For azobenzene, such a change in the UV–Vis spectra is evidence for *trans*-to-*cis* isomerization.[33] The *cis* isomeric form of azobenzene can return to its original *trans* state upon heating or placing in the dark. Fig. 9(b) reveals evidence for such a *cis*-to-*trans* isomerization phenomenon; when we placed our supramolecular complex in the dark, the spectra recovered to the original state by degrees. A quick *trans*-to-*cis* isomerization and slow *cis*-to-*trans* isomerization are typical of azobenzene-containing materials.[33] The UV-Vis spectrum of the blending thin film is shown in Fig. S6†

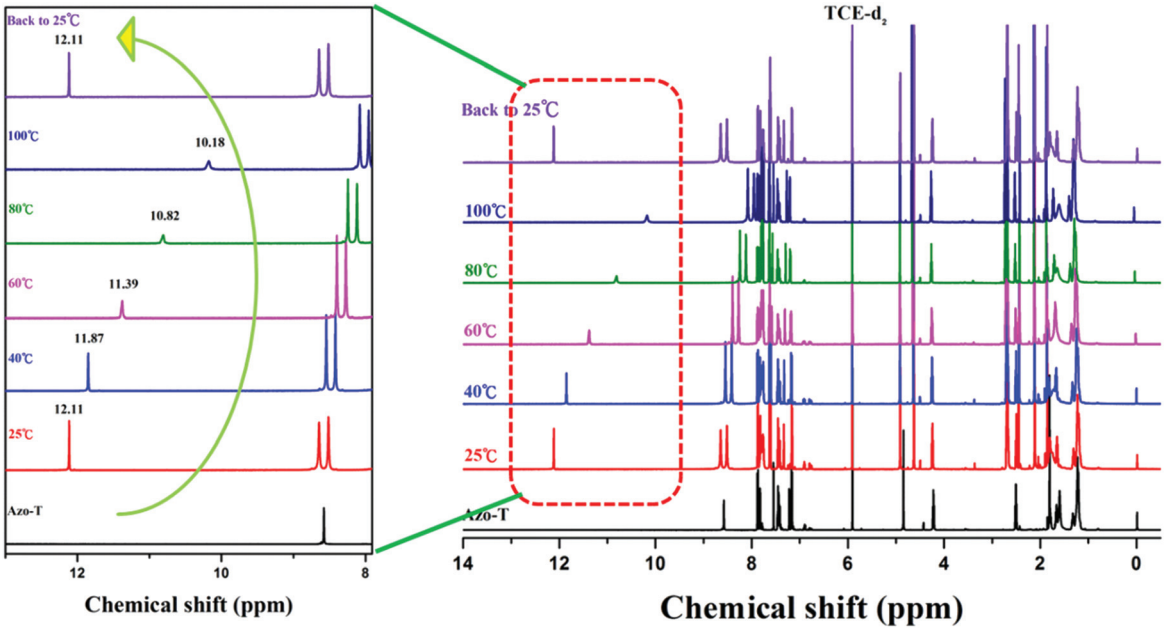

Fig. 8 ^{1}H NMR spectra of the Azo-T/SA-DAP supramolecular complex plotted with respect to temperature at a concentration of 10 wt%.

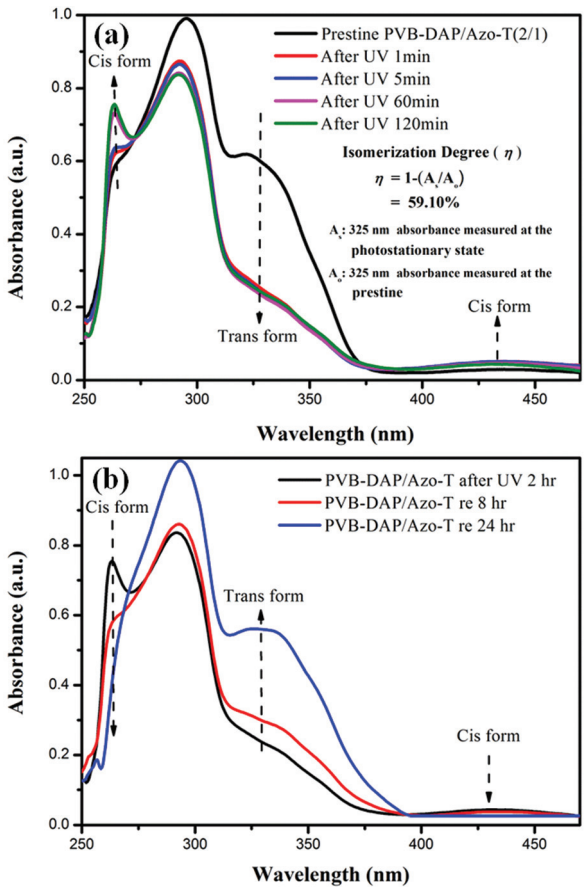

Fig. 9 UV-Vis spectra of the PVB-DAP/Azo-T supramolecular complex (a) before and after illumination with a UV lamp at 365 nm and (b) after standing in the dark at room temperature.

where the isomerization progress can still be observed with the gradually decreased π–π* absorption and slightly increased n–π* just as observed in the solution state. This result also claimed that the azo molecule in the blending system has enough ability to response the stimuli trigger. The combined results suggested that PVB-DAP/Azo-T formed a uniform photoresponsive complex. Such supramolecular crosslinked networks displaying photochemical reversibility may provide some degree of flexibility when designing smart materials.

Photoisomerization-induced control over surface properties

Preparing uniform (flat, homogeneous) films of pure azo-based small organic molecules for optical applications can be challenging because of their crystalline nature and ready aggregation. To solve this problem, here we used the amorphous homopolymer PVB-DAP, presenting complementary multiple hydrogen bonding motifs, for blending with Azo-T, thereby effectively avoiding self-aggregation of the azo-dye while, at the same time, significantly increasing its film-forming ability. Fig. 10(a) presents the resulting supramolecular thin films, displaying a range of colors, prepared at various blending ratios. Stimuli-responsive supramolecular complexes can undergo interesting transformations of their surface properties.[20] The measurement of WCAs can provide useful information when investigating the surface properties of organic films. The pristine static WCA for PVB-DAP/Azo-T (2/1) was 102°; it changed dramatically to 78° after UV irradiation at 365 nm for 3 h [Fig. 10(a)]. Thus, the hydrophilicity of the UV-exposed supramolecular thin film was greater than that of the non-exposed one. This finding, consistent with that in a previous report, confirms that illumination under UV light can lead to a variation in the dipole moment as a result of *trans*-to-

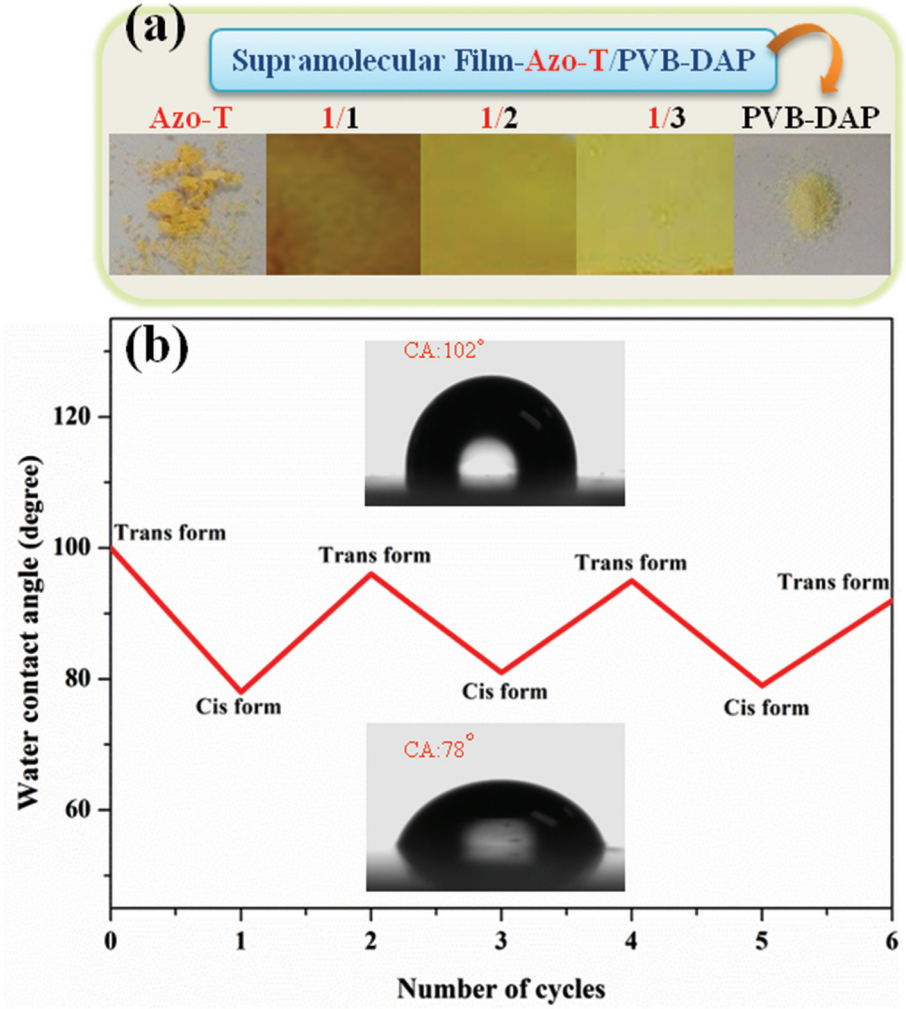

Fig. 10 (a) Comparison of the morphologies and colors of films of Azo-T, PVB-DAP, and their supramolecular complexes formed at various ratios. (b) WCAs of PVB-DAP/Azo-T supramolecular complexes after several cycles of UV irradiation and leaving in the dark.

cis isomerization.[20] The reason for WCA variation may be due to (1) the dipole moment change between *trans* and *cis* isomers of azobenzene. In the *trans* state, the azo molecules have smaller dipole moment and lower surface free energy because of the relative symmetrical molecular structure, thus leading to a higher WCA. However, after the UV-induced *trans* to *cis* isomerization process, the dipole moment increases significantly with the increase in the amount of the *cis* isomer.[20] In addition, the nitrogen atoms become easier to interact with polar groups such as water molecules. The isomerization of Azo-T may affect the entire surface properties of the supramolecular complex. (2) The surface roughness of thin film could be enhanced after the *cis* isomer formation. The isomerization involves a distance change of the Azo molecule from 9.0 Å (*trans*) to 5.5 Å (*cis*) and therefore results in the local contraction of the entire material.[20] Owing to the above reasons, a remarkable change in the surface geometry is often observed in the azo-containing materials. The conformational change can make a hydrophilic material become more hydrophilic, or make the hydrophobic material become hydrophilic. The wettability of such supramolecular thin films can return to the original state (*i.e.*, more hydrophobic) after thermal treatment or placing in the dark. Indeed, the resulting treated thin film displayed a WCA of 99°, close to the pristine value. Through three cycles of measurements we confirmed the reversibility of the switching of the supramolecular thin film; in other words, the supramolecular complex PVB-DAP/Azo-T exhibited photoresponsivity and photoreversibility. Thus, through simple blending, we could obtain a light-controllable supramolecular complex capable of effective tuning of its surface properties—a phenomenon we wished to exploit in the development of hydrophobic/hydrophilic patterns.

Photoinduced SRG fabrication

Because of its attractive photoresponsiveness, azobenzene has become a well-studied material for optical storage. For SRG fabrication, we first drop-coated a transparent thin film (thickness: 500 nm) of the PVB-DAP/Azo-T supramolecular complex

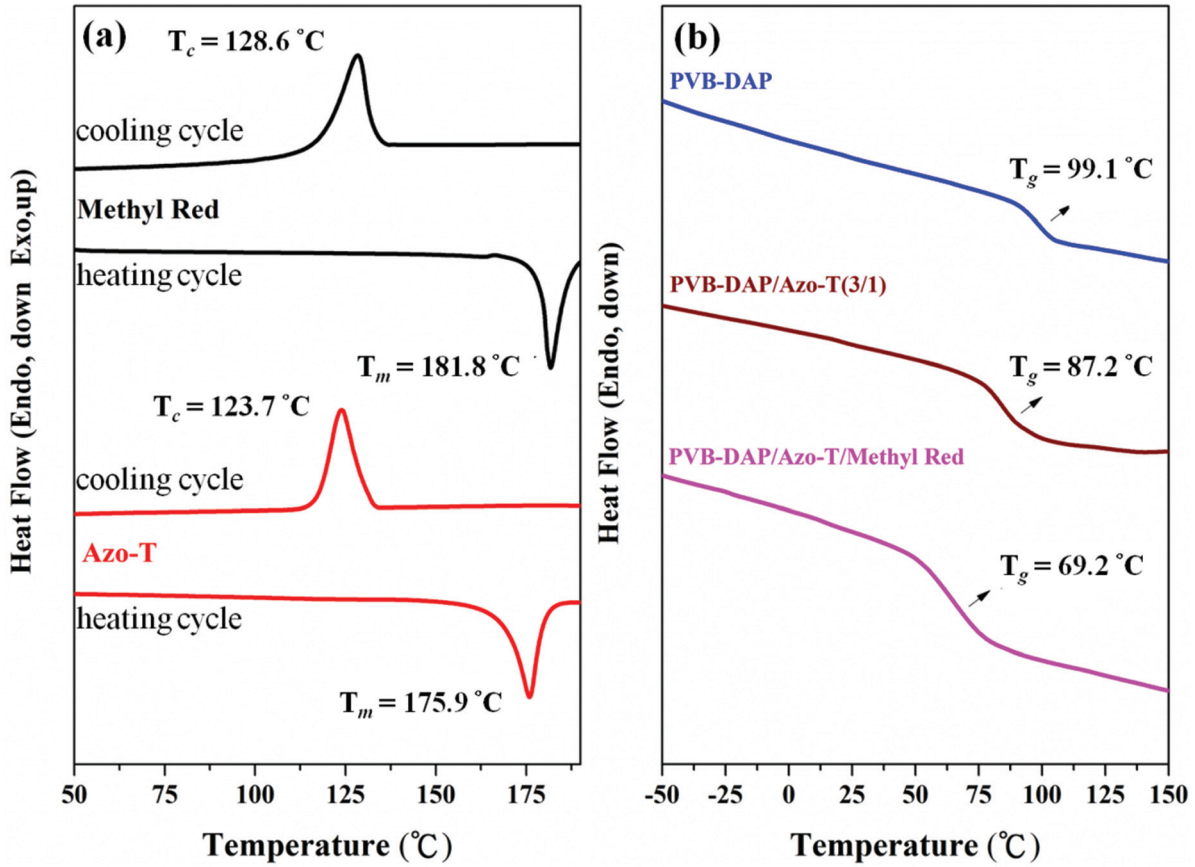

Fig. 11 (a) DSC cooling/heating cycles for methyl red (black curve) and Azo-T (red curve). (b) DSC thermograms for PVB-DAP, PVB-DAP/Azo-T, and PVB-DAP/Azo-T/methyl red recorded during the second heating cycle.

onto a clean glass substrate from the prepared solution. Here, we mixed methyl red, a commercial azo dye that provides good mass-transport, with our supramolecular complex to prepare the stock solution. Notably, methyl red is a crystalline material that readily forms aggregates in the solid state, so we were attempting to use the PVB-DAP/Azo-T supramolecular complex as the matrix for its dispersion. Fig. 11(a) reveals that methyl red displayed a value of T_c of 128.6 °C and a value of T_m of 181.8 °C, while for Azo-T these values were 123.7 and 175.9 °C, respectively; the appearance of signals for T_m and T_c indicates that both of these molecules are crystalline. Earlier, however, we noted that blending of Azo-T with PVB-DAP resulted in an amorphous supramolecular complex (Fig. 6), suggesting that the complementary hydrogen bonding plays an important role in its dispersion. Fig. 11(b) presents DSC traces for PVB-DAP, PVB-DAP/Azo-T(3/1), and PVB-DAP/Azo-T/methyl red during their second heating cycles. For PVB-DAP, a clear value of T_g appeared at 99.1 °C, as discussed above. The value of T_g for the PVB-DAP/Azo-T = 3/1 complex was 87.2 °C—slightly lower than that of the pure PVB-DAP polymer because of the plasticizing effect of the long alkyl chain of Azo-T. For the ternary PVB-DAP/Azo-T/methyl red = 3/1/1 blend complex, we observed a single value of T_g of 69.2 °C, implying the formation of a homogeneous complex through simple blending of these three materials. The miscible complex presumably arose from the favorable noncovalent interactions between Azo-T and methyl red, preventing the self-aggregation of methyl red and, thereby, decreasing the possibility of crystallization. The amorphous PVB-DAP could, therefore, behave as a matrix for the dispersion of Azo-T (through multiple hydrogen bonding interactions) and, consequently, methyl red. The value of T_g for the PVB-DAP/Azo-T/methyl red blend was much lower than that for the PVB-DAP/Azo-T complex because the presence of methyl red increased the free volume and made it easier for the polymer chains to move. Thus, DSC confirmed that methyl red could be dispersed well in our supramolecular complex—a criterion for successful film formation. Accordingly, we tested our homogeneous PVB-DAP/Azo-T/methyl red (3/1/1) system for SRG fabrication.

Scheme 2 illustrates the experimental setup we used for supramolecular SRG fabrication, using dye-doped PVB-DAP/Azo-T/methyl red (3/1/1) films as the recording material. We used the interference patterns established from two *p*-polarized laser beams to inscribe the SRGs. The supramolecular film displayed a clear spot after laser illumination at 532 nm for 30 min, indicating that a variation in the refractive index had

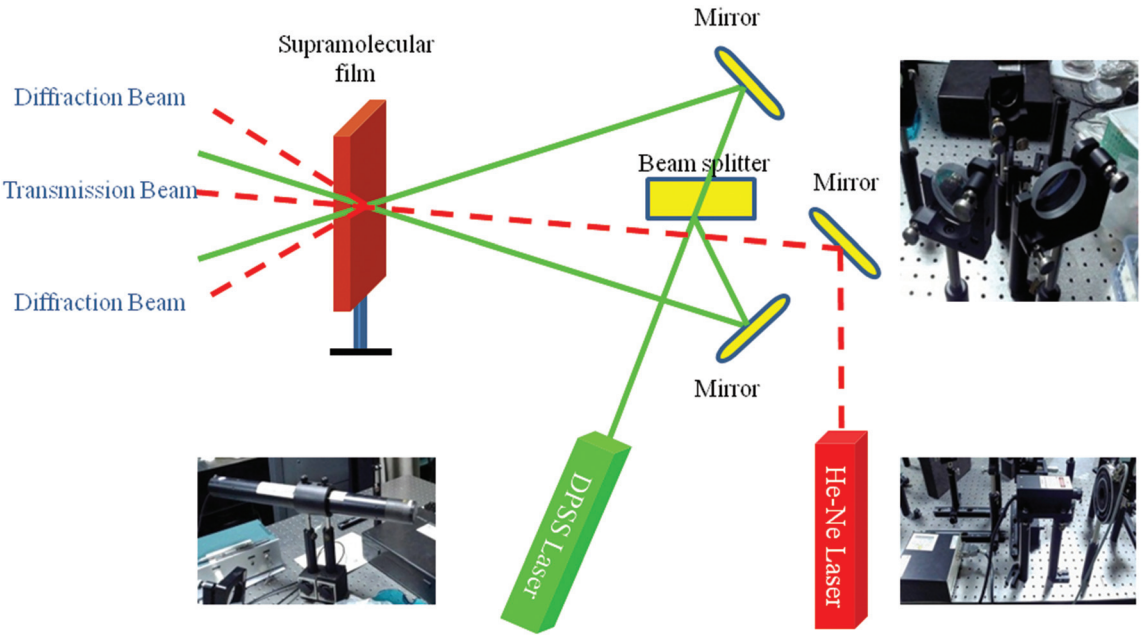

Scheme 2 Experimental set-up for fabrication of a supramolecular SRG film.

occurred [Fig. 12(a)]. Once the grating had formed, we observed a one-dimensional diffraction pattern with two first-order diffraction points [Fig. 12(b)]. Fig. 12(c) presents OM images of the profiles of the SRGs formed on the films. The gratings, measured one day after fabrication, were clearly revealed under OM. The grating spatial period was approximately 4.5 μm, with a surface-modulation depth of 7 nm, as calculated using AFM (Fig. S7†). For holographic storage, grating stability is a key issue. The application of traditional amorphous azo-polymers has been restricted because of their poor stability during storage; they have low values of T_g and tend to decompose over time.[17] In our system, however, we exploited the complementary multiple hydrogen bonding and other noncovalent interactions to form a homogeneous amorphous material. Unlike traditional amorphous azo-polymers, this supramolecular complex displayed a suitable value of T_g for holographic storage. The recorded film was fairly stable after storage for at least 6 months under an ambient atmosphere. The molecular orientation of its components was fixed because of their physical crosslinking, thereby enhancing the sustainability of resulting SRGs. Although gratified by the film's sufficient stability, it would be more useful if the material could be recycled and reused with a reproducible function from its original state. Accordingly, we heated the recorded film at 70 °C, a temperature slightly higher than its value of T_g. After heating for 1 h, the clear spot on the film disappeared and the film returned to its original state, accompanied by a zero-order diffraction pattern that was dominated by the incident beam (Fig. 13). Once the grating had been "erased," the +1 and −1 ordered diffraction points had disappeared. No cracking or aggregation crystals appeared after cooling to room temperature, indicating that the supramolecular interactions and amorphous nature remained consolidated in the entire film. When we exposed the film again to the 532 nm laser, +1 and −1 ordered diffraction points appeared with a clear spot on the film, identical to the situation after the first recording, confirming the responsivity and reversibility of our material. Such a "recordable" and "rewritable" stimuli-responsive complex, based on noncovalent interactions, should expand the applicability of supramolecular materials.

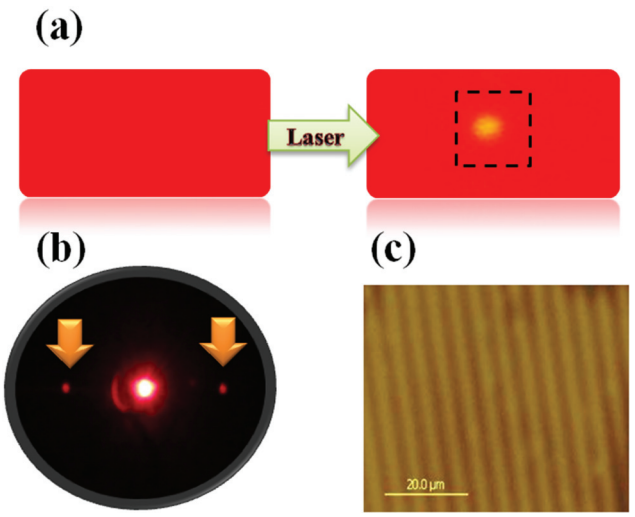

Fig. 12 Photographs of (a) the PVB-DAP/Azo-T/methyl red films before and after exposure to the laser light, (b) the diffraction patterns of SRGs probed with a 632 nm laser beam, and (c) the OM images of the recorded SRGs.

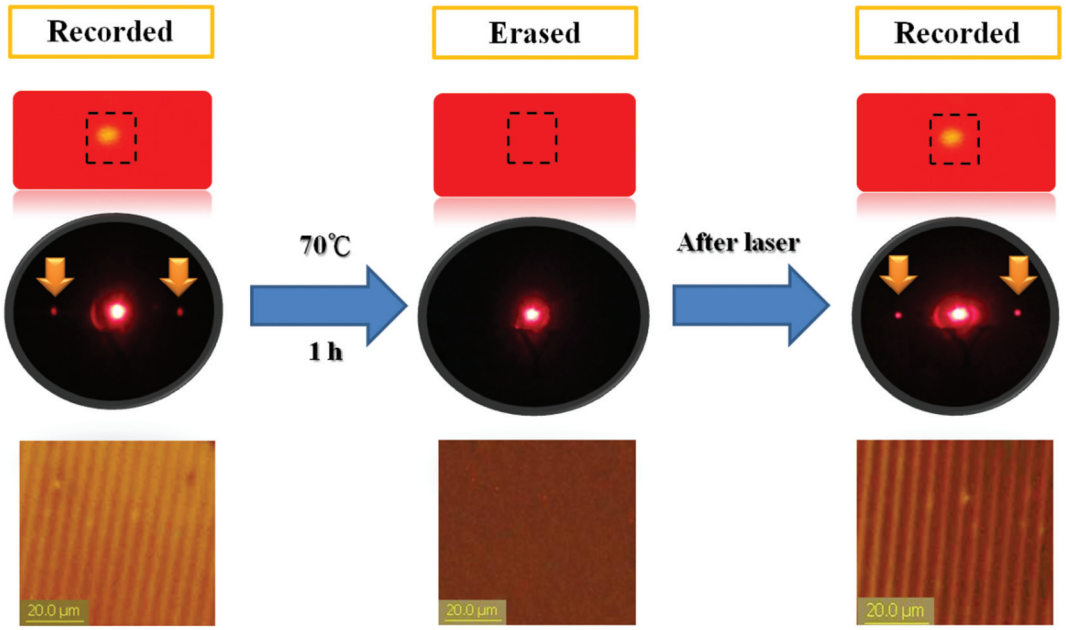

Fig. 13 Photographs and diffraction patterns of the supramolecular films after erasing and subsequent laser-recording.

Conclusion

We have prepared stimuli-responsive supramolecular materials through a facile synthesis and simple blending procedure. The DAP-functionalized polystyrene derivative PVB-DAP provided a matrix for the formation of supramolecular complexes with bioinspired T-/U-functionalized molecules, stabilized through directional and complementary multiple hydrogen bonding interactions. The supramolecular dye Azo-T, when complexed with PVB-DAP, underwent *trans*-to-*cis* isomerization upon irradiation with light. Control over the DAP-to-T ratio resulted in a homogeneous and amorphous material possessing a glass transition temperature suitable for SRG formation. We examined its photoresponsivity under UV and visible light, observing the spectral changes of the dye-doped polymeric material consistent with the photocontrollable behavior. The wettability of the PVB-DAP/Azo-T surface was also switchable and reversible, as evidenced from WCA measurements. We fabricated SRG micropatterns from our supramolecular complex combined with the commercially available chromophore methyl red. Noncovalent interactions effectively suppressed the crystallization of the azo dye and, therefore, allowed for successful fabrication of the SRG. This "recordable" and "rewritable" stimuli-responsive complex, stabilized through noncovalent interactions, might have applications in various optical systems (*e.g.*, for holographic storage), while also extending the possibilities of supramolecular development.

Acknowledgements

This study was supported financially by the Ministry of Science and Technology, Taiwan, under contracts MOST103-2221-E-110-079-MY3 and MOST102-2221-E-110-008-MY3. Special thanks to Mr L. Y. Wang of the National Sun Yat-Sen University for their assistance and advice regarding the fabrication of the holographic gratings.

Notes and references

1 (*a*) P. S. Stayton, T. Shimoboji, C. Long, A. Chilkoti, G. Ghen, J. M. Harris and A. S. Hoffman, *Nature*, 1995, **378**, 472; (*b*) P. M. Mendes, *Chem. Soc. Rev.*, 2008, **37**, 2512; (*c*) L. Su, Y. Zhao, G. S. Chen and M. Jiang, *Polym. Chem.*, 2012, **3**, 1560; (*d*) K. Liu, Y. L. Liu, Y. X. Yao, H. X. Yuan, S. Wang, Z. Q. Wang and X. Zhang, *Angew. Chem., Int. Ed.*, 2013, **52**, 8285; (*e*) Y. Han, J. J. Li, M. H. Zan, S. Z. Luo, Z. S. Ge and S. Y. Liu, *Polym. Chem.*, 2014, **5**, 3707.

2 (*a*) D. H. Carey, S. J. Grunzinger and G. S. Ferguson, *Macromolecules*, 2000, **33**, 8802; (*b*) J. T. Koberstein, *J. Polym. Sci., Part B: Polym. Phys.*, 2004, **42**, 29426; (*c*) I. Luzinov, S. Minko and V. V. Tsukruk, *Soft Matter*, 2008, **4**, 714; (*d*) Z. S. Ge, J. M. Hu, F. H. Huang and S. Y. Liu, *Angew. Chem., Int. Ed.*, 2009, **121**, 1830; (*e*) X. J. Liao, G. S. Chen, X. X. Liu, W. X. Chen, F. Chen and M. Jiang, *Angew. Chem., Int. Ed.*, 2010, **49**, 4409.

3 (*a*) F. Zhou, W. M. Shu, M. E. Welland and W. T. S. Huck, *J. Am. Chem. Soc.*, 2006, **128**, 5326; (*b*) A. Valiaev, N. I. Abu-Lail, D. W. Lim, A. Chilkoti and S. Zauscher, *Langmuir*, 2007, **23**, 339.

4 (*a*) Y. Liu, L. Mu, B. H. Liu and J. L. Kong, *Chem. – Eur. J.*, 2005, **11**, 2622; (*b*) C. Alexander and K. M. Shakesheff, *Adv. Mater.*, 2006, **18**, 3321; (*c*) G. S. Chen and M. Jiang, *Chem. Soc. Rev.*, 2011, **40**, 2254; (*d*) X. L. Hu and S. Y. Liu, *Dalton*

Trans., 2015, **44**, 3904; (*e*) X. L. Hu, G. H. Liu, Y. Li, X. R. Wang and S. Y. Liu, *J. Am. Chem. Soc.*, 2015, **137**, 362.

5 (*a*) W. H. Binder and R. Sachsenhofer, *Macromol. Rapid Commun.*, 2007, **28**, 15; (*b*) K. Matyjaszewski, *Macromolecules*, 2012, **45**, 4015; (*c*) Y. Yao, Y. Wang and F. H. Huang, *Chem. Sci.*, 2014, **5**, 4312.

6 (*a*) A.-V. Ruzette and L. Leibler, *Nat. Mater.*, 2005, **4**, 19; (*b*) Z. S. Ge and S. Y. Liu, *Chem. Soc. Rev.*, 2013, **42**, 7289; (*c*) S. T. Hemp, A. E. Smith, W. C. Bunyard, M. H. Rubinstein and T. E. Long, *Polymer*, 2014, **55**, 2325.

7 H. C. Kolb, M. G. Finn and K. B. Sharpless, *Angew. Chem., Int. Ed.*, 2001, **40**, 2004.

8 (*a*) S. Rieth, C. Baddeley and J. D. Badjic, *Soft Matter*, 2007, **3**, 137; (*b*) D. Klinger, M. J. Robb, J. M. Spruell, N. A. Lynd, C. J. Hawkerab and L. A. Connal, *Polym. Chem.*, 2013, **4**, 5038; (*c*) Y. L. Liu, Z. Q. Wang and X. Zhang, *Chem. Soc. Rev.*, 2012, **41**, 5922.

9 (*a*) L. J. Prins, D. N. Reinhoudt and P. Timmerman, *Angew. Chem., Int. Ed.*, 2001, **40**, 2382; (*b*) A. Priimagi, K. Lindfors, M. Kaivola and P. Rochon, *ACS Appl. Mater. Interfaces*, 2009, **1**, 1183; (*c*) A. Kokil, T. Saito, W. Depolo, C. L. Elkins, G. L. Wilkes and T. E. Long, *J. Macromol. Sci., Pure Appl. Chem.*, 2011, **48**, 1016; (*d*) D. J. Broer, C. M. W. Bastiaansen, M. G. Debije and A. P. H. J. Schenning, *Angew. Chem., Int. Ed.*, 2012, **51**, 7102; (*e*) S. Cheng, M. Zhang, N. Dixit, B. R. Moore and T. E. Long, *Macromolecules*, 2012, **45**, 805; (*f*) D. A. Leigh, C. C. Robertson, A. M. Z. Slawin and P. I. T. Thomson, *J. Am. Chem. Soc.*, 2013, **135**, 9939.

10 (*a*) L. Brunsveld, B. J. B. Folmer, E. W. Meijer and R. P. Sijbesma, *Chem. Rev.*, 2001, **101**, 4071; (*b*) G. B. W. L. Ligthart, H. Ohkawa, R. P. Sijbesma and E. W. Meijer, *J. Am. Chem. Soc.*, 2005, **127**, 810; (*c*) S. T. Hemp and T. E. Long, *Macromol. Biosci.*, 2012, **12**, 29; (*d*) J. Xu, H. D. Yu, L. L. Yang, G. L. Wu, Z. Q. Wang, D. Wang and X. Zhang, *Chem. Sci.*, 2015, **6**, 4907.

11 (*a*) F. J. M. Hoeben, P. Jonkheijm, E. W. Meijer and A. P. H. J. Schenning, *Chem. Rev.*, 2005, **105**, 1491; (*b*) A. Bertrand, F. Lortie and J. Bernard, *Macromol. Rapid Commun.*, 2012, **33**, 2062; (*c*) X. X. Tan, L. L. Yang, Y. L. Liu, Z. H. Huang, H. Yang, Z. Q. Wang and X. Zhang, *Polym. Chem.*, 2013, **4**, 5378.

12 S. L. Sin, L. H. Gan, X. Hu, K. C. Tam and Y. Y. Gan, *Macromolecules*, 2005, **38**, 3943.

13 (*a*) J. Zou, F. G. Tao and M. Jiang, *Langmuir*, 2007, **23**, 12791; (*b*) X. Y. Zheng, D. Wang, Z. G. Shuai and X. Zhang, *J. Phys. Chem. B*, 2012, **116**, 823; (*c*) D. Patra, H. Zhang, S. Sengupta and A. Sen, *ACS Nano*, 2013, **7**, 7674.

14 E. Blasco, M. Piñol and L. Oriol, *Macromol. Rapid Commun.*, 2014, **35**, 1090.

15 (*a*) P. Rochon, E. Batalla and A. Natansohn, *Appl. Phys. Lett.*, 1995, **66**, 136; (*b*) T. Yamamoto, M. Hasegawa, A. Kanazawa, T. Shiono and T. Ikeda, *J. Phys. Chem. B*, 1999, **103**, 9873.

16 (*a*) S. Hvilsted, C. Sánchez and R. Alcala, *J. Mater. Chem.*, 2009, **19**, 6641; (*b*) F. K. Bruder, R. Hagen, T. Roelle, M. S. Weiser and T. Faecke, *Angew. Chem., Int. Ed.*, 2011, **50**, 4552.

17 A. Natansohn and P. Rochon, *Chem. Rev.*, 2002, **102**, 4139.

18 (*a*) C. Barrett, A. Natansohn and P. Rochon, *J. Phys. Chem.*, 1996, **100**, 8836; (*b*) V. Borger, S. Pohle, O. Kulikovska, K. Gharaggozloo-Hubmann, J. Stumpe and H. Menzel, *Macromol. Symp.*, 2009, **275–276**, 257.

19 J. Vapaavuori, A. Priimagi and M. Kaivola, *J. Mater. Chem.*, 2010, **20**, 5260.

20 (*a*) J. J. Delang, J. M. Robertson and I. Woodward, *Proc. R. Soc. London, Ser. A*, 1939, **171**, 398; (*b*) G. S. Kumar and D. C. Neckers, *Chem. Rev.*, 1989, **89**, 1915; (*c*) B. Tylkowski, S. Peris, M. Giamberini, R. Garcia-Valls, J. A. Reina and J. C. Ronda, *Langmuir*, 2010, **26**, 14821; (*d*) I. H. Lin, C. C. Cheng, K. F. Li, J. K. Chen, C. W. Chiu and F. C. Chang, *Polym. Chem.*, 2014, **5**, 702.

21 (*a*) J. B. Carroll, B. L. Frankamp and V. M. Rotello, *Chem. Commun.*, 2002, 1892; (*b*) J. B. Carroll, A. J. Waddon, H. Nakade and V. M. Rotello, *Macromolecules*, 2003, **36**, 6289; (*c*) S. H. Lee, M. Ouchi and M. Sawamoto, *J. Polym. Sci., Part A: Polym. Chem.*, 2013, **51**, 4498.

22 F. Ilhan, M. Gray and V. M. Rotello, *Macromolecules*, 2001, **34**, 2597.

23 Z. Sideratou, D. Tsiourvas, C. M. Paleos, E. Peppas, J. Anastassopoulou and T. Theophanides, *J. Mol. Struct.*, 1999, **484**, 91.

24 (*a*) Y. Kyogoku, R. C. Lord and A. Rich, *J. Am. Chem. Soc.*, 1967, **89**, 496; (*b*) Y. Dahman, J. E. Puskas, A. Margaritis, Z. Merali and M. Cunningham, *Macromolecules*, 2003, **36**, 2198.

25 J. H. Wang, O. Altukhov, C. C. Cheng, F. C. Chang and S. W. Kuo, *Soft Matter*, 2013, **9**, 5196.

26 (*a*) M. Aubin and R. E. PrudHomme, *Polym. Eng. Sci.*, 1998, **21**, 1355; (*b*) I. M. Kalogeras and W. Brostow, *J. Polym. Sci., Part B: Polym. Phys.*, 2013, **51**, 4498.

27 A. Concellón, E. Blasco, M. Piñol, L. Oriol, I. Díez, C. Berges, C. S. Somolinos and R. Alcalá, *J. Polym. Sci., Part A: Polym. Chem.*, 2014, **52**, 3173.

28 C. C. Cheng, C. F. Huang, Y. C. Yen and F. C. Chang, *J. Polym. Sci., Part A: Polym. Chem.*, 2008, **19**, 6416.

29 (*a*) I. H. Lin, C. C. Cheng, Y. C. Yen and F. C. Chang, *Macromolecules*, 2010, **43**, 1245; (*b*) I. H. Lin, C. C. Cheng, C. W. Huang, M. C. Liang, J. K. Chen, F. H. Ko, C. W. Chu, C. F. Huang and F. C. Chang, *RSC Adv.*, 2013, **3**, 12598; (*c*) M. Tamami, S. T. Hemp, K. Zhang, M. Zhang, R. B. Moore and T. E. Long, *Polymer*, 2013, **54**, 1588.

30 (*a*) S. H. Cellman, G. P. Dado, C. B. Liang and B. R. Adam, *J. Am. Chem. Soc.*, 1991, **113**, 1164; (*b*) L. Fielding, *Tetrahedron*, 2000, **56**, 6151; (*c*) N. Mesplet, P. Morin and J. P. Ribet, *Eur. J. Pharm. Biopharm.*, 2005, **59**, 523.

31 E. Kolomiets, E. Buhler, S. J. Candau and J. M. Lehn, *Macromolecules*, 2006, **39**, 1173.

32 (*a*) O. Uzun, A. Sanyal, H. Nakade, R. J. Thibault and V. M. Rotello, *J. Am. Chem. Soc.*, 2004, **126**, 14773; (*b*) C. C. Cheng, Y. C. Yen and F. C. Chang, *RSC Adv.*, 2011, **1**, 1190.

33 Z. Xie, H. F. He, Y. H. Deng, X. G. Wang and C. Y. Liu, *J. Mater. Chem. C*, 2013, **1**, 1791.

